Article

Material Exchange Property of Organo Lead Halide Perovskite with Hole-Transporting Materials

Seigo Ito [1],*, Shusaku Kanaya [1], Hitoshi Nishino [2], Tomokazu Umeyama [3] and Hiroshi Imahori [3,4]

[1] Department of Materials and Synchrotron Radiation Engineering, Graduate School of Engineering, University of Hyogo, 2167 Shosha, Himeji, Hyogo, 671-2201, Japan;
E-Mail: ej15m007@steng.u-hyogo.ac.jp

[2] Energy Technology Laboratories, Osaka Gas Co., Ltd., Osaka 554-0051, Japan;
E-Mail: nishino@osakagas.co.jp

[3] Department of Molecular Engineering, Graduate School of Engineering, Kyoto University, Kyoto 615-8510, Japan; E-Mails: umeyama@scl.kyoto-u.ac.jp (T.U.); imahori@scl.kyoto-u.ac.jp (H.I.)

[4] Institute for Integrated Cell-Material Sciences (WPI-iCeMS), Kyoto University, Kyoto 615-8510, Japan

Author to whom correspondence should be addressed; E-Mail: itou@eng.u-hyogo.ac.jp

Abstract: Using X-ray diffraction (XRD), it was confirmed that the deposition of hole-transporting materials (HTM) on a $CH_3NH_3PbI_3$ perovskite layer changed the $CH_3NH_3PbI_3$ perovskite crystal, which was due to the material exchanging phenomena between the $CH_3NH_3PbI_3$ perovskite and HTM layers. The solvent for HTM also changed the perovskite crystal. In order to suppress the crystal change, doping by chloride ion, bromide ion and 5-aminovaleric acid was attempted. However, the doping was unable to stabilize the perovskite crystal against HTM deposition. It can be concluded that the $CH_3NH_3PbI_3$ perovskite crystal is too soft and flexible to stabilize against HTM deposition.

Keywords: CuSCN, cupper thiocyanate, inter diffusion, stability, material exchanging

1. Introduction

After the finding of the organo lead halide perovskite solar cell by the groups of Miyasaka, Snaith, Park and Grätzel [1–4], it has received significant attention in the last five years with improvement of the conversion efficiency from 3% [1] to a certified value of 20.1% [5]. The organo lead halide

perovskite solar cells had been thought to be a solid-state device. However, with the recent efforts of scientist, it has emerged that the organo lead halide perovskite is an ion-conductive semiconductor [6,7]. Although the organo lead halide layer can give a clear perovskite crystal structure, as revealed by X-ray diffraction (XRD), it is just a moisture-sensitive and the most chemically-soluble salt.

Basically, printed devices should be deposited on a hard-soluble material to an easy-soluble one. Otherwise, the former material can be dissoluble into the latter one. For example, although CuSCN hole-transporting material (HTM) can work on the $CH_3NH_3PbI_3$ perovskite layer to be a solar cell [8], the CuSCN and $CH_3NH_3PbI_3$ perovskite can diffuse into each other and make a short circuit [8,9]. In order to improve the conversion efficiency of perovskite solar cells, this phenomena is a critical issue. In this paper, we have disclosed the chemical effects on the $CH_3NH_3PbI_3$ perovskite layer, which has been investigated by X-ray diffraction (XRD). The materials deposited on the $CH_3NH_3PbI_3$ perovskite layer were solvents for HTM (chlorobenzene and propyl sulfide) and the HTM layer itself 2,2',7,7'-Tetrakis-(*N,N*-di-*p*-methoxyphenylamine)-9,9'-spirobifluorene (spiro-OMeTAD with dopants and CuSCN). In order to enhance the strength of the $CH_3NH_3PbI_3$ perovskite crystal, dopants of halide (chloride and bromide) and 5-aminovaleic acid, which can make a two-dimensional (2D) perovskite layer to enhance crystallinity and stability [10–12], were also adopted for this study.

2. Experiments

A commercial TiO_2-nanocrystalline paste (the code name "PST-18NR", $d = 18$ nm, JGC Catalysts and Chemicals Ltd., Kawasaki, Japan) was diluted to one-tenth with ethanol for spin-coating. Porous TiO_2 layers were fabricated by a spin-coating method (5000 rpm for 30 s) on glass substrates, which were washed by an ultrasonic water bath with detergent and a UV/O_3 system beforehand and annealed at 500 ℃ for 30 min.

By a one-step process, 4 types of organo lead halide perovskite crystals were fabricated using *N,N*-dimethylformamide (DMF): (1) $CH_3NH_3PbI_3$ ($CH_3NH_3I:PbI_2$ = 2:1, in DMF); (2) $CH_3NH_3PbCl_xI_{3-x}$ ($CH_3NH_3I:CH_3NH_3Cl:PbI_2$ = 1:1:1, in DMF); (3) $CH_3NH_3PbBr_xI_{3-x}$ (methylammonium iodide (MAI):PbI_2:$PbBr_2$ = 2:0.9:0.1, in DMF); and (4) $(HOOC(CH_2)_4NH_3)_x(CH_3NH_3)_{1-x}PbI_3$ (MAI:5-aminovaleric acid(5-AVAI):PbI_2 = 25:1:25, in DMF). The amount of Pb in DMF was 1.2 M, consistently. Each solution was stirred at 70 ℃ and then coated on the mesoporous TiO_2 film by spin-coating at 2000 rpm for 30 s (5-s acceleration), followed by annealing at 100 ℃ for (1) to (3) and at 50 ℃ for (4).

For the two-step process $CH_3NH_3PbI_3$ perovskite deposition, 1.2 M of PbI_2 was dissolved in 2 mL of *N,N*-dimethylformamide by stirring at 70 ℃, deposited on the mesoporous TiO_2 film by spin-coating at 6500 rpm for 20 s and dried at 100 ℃ for 30 min. Then, the TiO_2/PbI_2 film was dipped into a solution of CH_3NH_3I in 2-propanol (10 mg/mL) for 20 s and then rinsed with 2-propanol and spun to dry at 4000 rpm for 8 s (2-s acceleration). Finally, the deposited $CH_3NH_3PbI_3$ film was dried on a hotplate at 70 ℃ for 30 min.

A CuSCN hole conductor was deposited on $CH_3NH_3PbI_3$ layers by the doctor blading method at 65 ℃ (the CuSCN solution was prepared by dissolving 6 mg of CuSCN (Kishida Chemical Co. Ltd., Osaka, Japan) into 1 mL of propyl sulfide) [6,7,11]. 2,2',7,7'-Tetrakis-(*N,N*-di-*p*-methoxyphenylamine)-9, 9'-spirobifluorene (spiro-OMeTAD, Merck Japan, Tokyo, Japan) was deposited as an organic hole

conducting material (HTM) with doping materials (4-*tert*-butylpyridine (TBP), lithium bis(trifluoromethylsulfonyl)imide (LiTFSI) and tris(2-(1H-pyrazol-1-yl)-4-*tert*-butylpyridine)cobalt(III) tris(bis(trifluoromethylsulfonyl) imide) in chlorobenzene [13]. The organic HTM solution was deposited using the spin-coating method at 4000 rpm. The crystal structures were characterized using X-ray diffraction (Miniflex II, Rigaku, Tokyo, Japan) with Cu Kα radiation.

3. Results and Discussions

At first, the solvent-rinsing effect on $CH_3NH_3PbI_3$ perovskite crystal variation was considered before the HTM deposition itself. Figure 1 shows the XRD patterns of the $CH_3NH_3PbI_3$ perovskite crystal after spin-coating chlorobenzene (solvent of spiro-OMeTAD) and propyl sulfide (solvent of CuSCN) on one-step processed $CH_3NH_3PbI_3$ perovskite layers. The original $CH_3NH_3PbI_3$ perovskite crystal showed the XRD peak at 13.7 ° and 468 counts. Although the intensity of XRD counts was related to the measurement setup, the height between the samples can be compared to discuss the variation of crystal structures using the same system consistently. It was surprising that just spin-coating chlorobenzene, which has been used for the spiro-OMeTAD deposition as an inert solvent against the $CH_3NH_3PbI_3$ perovskite crystal, can shift the peak to a higher angle and reduce the height of the XRD peak to half of the original one. The XRD peak shift to a higher angle means that the crystal lattice became shorter. This phenomenon may be due to the extraction of remaining DMF in the perovskite layer to chlorobenzene, which was explained as the "antisolvent method" published by Xiao *et al.* [14]. This result informs us that the remaining DMF in the perovskite crystal after the annealing procedure can be removed, because of the softness of the $CH_3NH_3PbI_3$ perovskite crystal [6,7]. In contrast, propyl sulfide (the solvent of CuSCN) did not change the XRD peak of the $CH_3NH_3PbI_3$ perovskite crystal, but reduced the XRD peak height. Since solvents (chlorobenzene and propyl sulfide) reduce the XRD peak of the $CH_3NH_3PbI_3$ perovskite crystal, the deposition of HTM by spin-coating can reduce the crystallinity of $CH_3NH_3PbI_3$ perovskite due to the solvent effect.
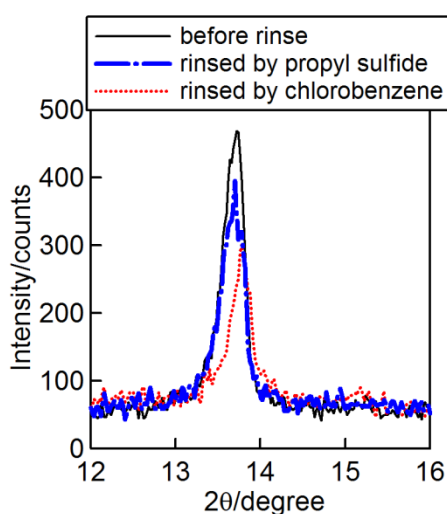

Figure 1. XRD patterns of one-step-processed $CH_3NH_3PbI_3$ perovskite layers varied by solvent rinsing on the perovskite layer.

Figure 2 shows the XRD patterns of one-step-processed $CH_3NH_3PbI_3$ perovskite crystals with HTM layers. The peak at 15.8° represents the crystal of the CuSCN layer. It was surprising that CuSCN deposition enhanced the crystallinity of $CH_3NH_3PbI_3$ perovskite, which may be due to the Cu^+-ion and SCN^--ion migration into $CH_3NH_3PbI_3$ perovskite, resulting in the enhancement of the perovskite crystal. Actually, $CH_3NH_3Pb(SCN)_2I$ can also be a perovskite solar cell, effectively [15]. In contrast, the XRD pattern of $CH_3NH_3PbI_3$ perovskite did not change with spiro-OMeTAD deposition. Hence, it was considered that the solvent of spiro-OMeTAD (chlorobenzene) can shift the XRD peak position to the higher angle, but that the dopant (which may be lithium ion and TBP) can shift it back to the original position, due to the special phenomena of material migration in the $CH_3NH_3PbI_3$ perovskite crystal [6,7].

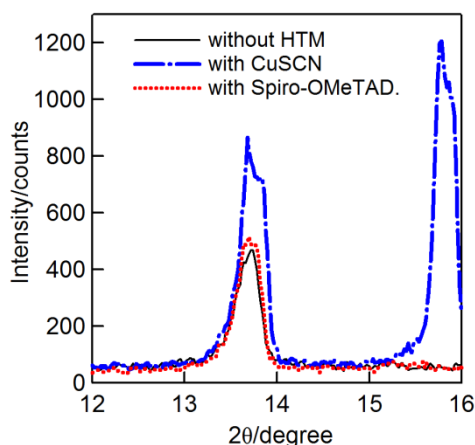**Figure 2.** XRD patterns of one-step-processed $CH_3NH_3PbI_3$ perovskite layers varied by hole-conducting materials (HTM) on the perovskite layer. 2,2',7,7'-Tetrakis-(*N,N*-di-*p*-methoxyphenylamine)-9,9'-spirobifluorene is represented as "spiro-OMeTAD".

Figure 3 shows the XRD patterns of the two-step deposition of the $CH_3NH_3PbI_3$ perovskite crystal with the HTM layer. Due to the procedure of the two-step sequential deposition of the PbI_2 crystal into methylammonium iodide solution, some part of the PbI_2 can remain [9]. Although the CuSCN XRD peak can remain on the one-step deposited $CH_3NH_3PbI_3$ (15.8°, in Figure 2), it was found that the peak of CuSCN vanished on the two-step-deposited $CH_3NH_3PbI_3$ perovskite layer, which may be due to the attack of the excess amount of iodide ion from the PbI_2 layer on the CuSCN crystal. It was also proposed that the thiocyanate ion (SCN^-) can migrate to the PbI_2 layer and can be exchanged with the ion with iodide ion (I^-) to form the $CH_3NH_3Pb(SCN)_2I$ perovskite crystal, resulting in the emission of the iodide ion to the CuSCN layer to be some amorphous phase. Hence, we can observe the shift of the PbI_2 layer. Moreover, the CuSCN can shift the XRD pattern of $CH_3NH_3PbI_3$ perovskite to a higher angle and lower intensity. Therefore, CuSCN can be mixed with the $CH_3NH_3PbI_3$ perovskite crystal effectively. In contrast, the effect of spiro-OMeTAD coating on the two-step-processed perovskite is also quite significant, because the spiro-OMeTAD coating causes the peak of PbI_2 to vanish and can shift the perovskite peak to the same position with the one-step-deposited $CH_3NH_3PbI_3$ perovskite. This PbI_2 decomposition may be due to the attack of the lithium ion and TBP on the PbI_2 crystal.

It was confirmed that the $CH_3NH_3PbI_3$ perovskite crystal was quite soft, and it was easy to change the lattice with the deposition of the HTM layer. In order to stabilize the $CH_3NH_3PbI_3$ perovskite crystal,

we have attempted doping with other halogens (chloride and bromide) and 5-aminovaleric acid (AVA) in the $CH_3NH_3PbI_3$ perovskite crystal.

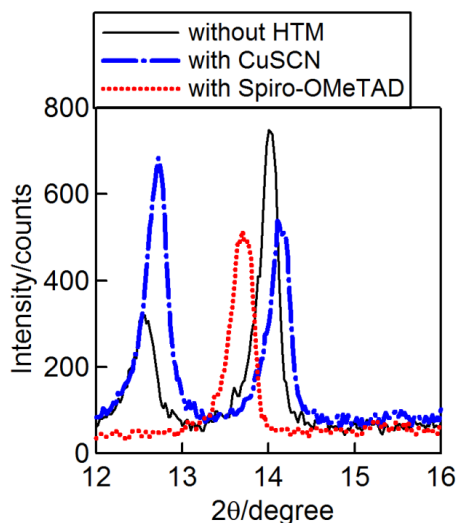**Figure 3.** XRD patterns of the two-step-processed $CH_3NH_3PbI_3$ perovskite layers varied by hole-conducting materials (HTM) on the perovskite layer. 2,2',7,7'-Tetrakis-(*N,N*-di-*p*-methoxyphenylamine)-9,9'-spirobifluorene is represented as "spiro-OMeTAD".

Figure 4 shows the doping effects of Cl^- and Br^- ions on the $CH_3NH_3PbI_3$ perovskite and HTM layers. Although there are some publication about Cl^- and Br^- ions, which can enhance the crystallinity and stability of the $CH_3NH_3PbI_3$ perovskite crystal [10,11], Figure 4 suggests that Cl^- and Br^- ions cannot stabilize the $CH_3NH_3PbI_3$ crystal against HTM deposition. It was confirmed that the doping of Cl^- and Br^- ions can greatly reduce or cause the XRD peak of CuSCN to vanish, which should arise around 15.8 ° (as in Figure 2). Actually, the chloride ion can improve the crystallinity of $CH_3NH_3PbI_3$ perovskite with over 10,000 counts of XRD (Figure 4a). However, the HTM deposition of spiro-OMeTAD or CuSCN can reduce the XRD intensity and shift the position of the XRD peak. Specially, the deposition of spiro-OMeTAD can reduce the XRD peak of the $CH_3NH_3PbI_3$ perovskite crystal very significantly. With the bromide ion, the XRD peak of $CH_3NH_3PbI_3$ perovskite can improve with the incorporation of CuSCN (Figure 4b). The vanishing effect of the CuSCN peak by the chloride ion is stronger than that by the bromide ion.

Figure 5 shows the XRD patterns of the 5-AVA-doped $CH_3NH_3PbI_3$ perovskite crystal by spin-coating deposition. Although only one XRD peak of 5-AVA-doped $CH_3NH_3PbI_3$ perovskite was observed below 10 ° in the literature [12], three intense peaks from 6 ° to 10 ° were observed as the 2D $CH_3NH_3PbI_3$ perovskite crystal. The difference from the published results may be due to the fabrication methods: spin-coating and drop casting. Without HTM, the peaks of the three-dimensional (3D) $CH_3NH_3PbI_3$ perovskite crystal (at 13.9 °) and PbI_2 (at 12.9 °) were quite small. Adding CuSCN HTM, the peak position of the 2D $CH_3NH_3PbI_3$ perovskite crystal did not change, but the peak height was decreased to less than half. At the same time, the peaks of the 3D $CH_3NH_3PbI_3$ perovskite crystal (at 13.9 °) and PbI_2 (at 12.5 °) were increased significantly. The peak height of the 3D $CH_3NH_3PbI_3$ perovskite crystal became very close to the one-step-processed $CH_3NH_3PbI_3$ perovskite. Adding spiro-OMeTAD, in contrast, the peak position of the 2D $CH_3NH_3PbI_3$ perovskite crystal was shifted to the lower angle, and

the peak height was increased. Although the peaks of the 3D CH₃NH₃PbI₃ perovskite crystal and PbI₂ were increased, the increment by spiro-OMeTAD was half of that by CuSCN. Hence, spiro-OMeTAD did not change the 2D CH₃NH₃PbI₃ perovskite crystal, but some of the contents (maybe the lithium ion and TBP) can be inserted between the 2D CH₃NH₃PbI₃ perovskite layers, which can be explained by the peak shift of 2D perovskite to the lower angle. Such a 2D perovskite layer has stability against moisture [12,16]. However, it was confirmed that such a 2D perovskite also can be changed by HTM deposition.
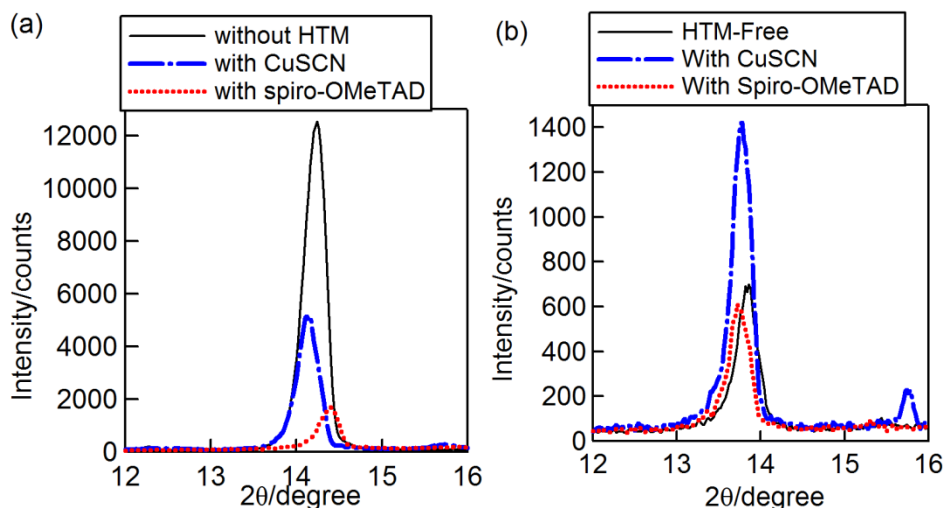

Figure 4. XRD patterns of one-step-processed CH₃NH₃PbI₃ perovskite layers with chloride and/or bromide doping, varied by hole-conducting materials (HTM) on the perovskite layer with chloride doping (**a**) and with bromide doping (**b**). 2,2',7,7'-Tetrakis-(*N,N*-di-*p*-methoxyphenylamine)-9,9'-spirobifluorene is represented as "spiro-OMeTAD".
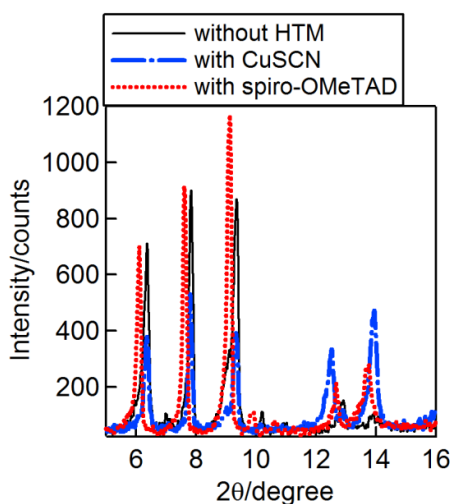

Figure 5. XRD patterns of the one-step-processed CH₃NH₃PbI₃ perovskite layers with 5-aminovaleric acid (5-AVA) doping, varied by hole-conducting materials (HTM) on the perovskite layer. 2,2',7,7'-Tetrakis-(*N,N*-di-*p*-methoxyphenylamine)-9,9'-spirobifluorene is represented as "spiro-OMeTAD".

However, it was found that the resulting PbI_2 layer from the 2D $CH_3NH_3PbI_3$ perovskite layer has higher stability than the 3D perovskite crystal. Figure 6 shows a picture of PbI_2 layers after water deposition (with different pH) of $CH_3NH_3PbI_3$ perovskite layers (with/without 5-AVA doping). The $CH_3NH_3PbI_3$ perovskite layers with/without 5-AVA doping have been decomposed to PbI_2 by dipping in water. When the amount of eluted Pb in the water was measured, no elution of Pb was observed using neutral water (pH = 7). However, alkaline water solution (pH = 12 of NaOH aq. solution) dissolved the $CH_3NH_3PbI_3$ perovskite layers completely. The observed amounts of Pb ion using $CH_3NH_3PbI_3$ perovskite layers with/without 5-AVA doping were 800 mg/m^2 and 725 mg/m^2, respectively. This small variation may be due to the difference of thickness after the 5-AVA doping. The significant difference of doping was confirmed using acidic water solution (pH = 2, HCl aq. solution). The 5-AVA doping can enhance the stability of the PbI_2 crystal against acidic water solution. This kind of effort to suppress the leakage of Pb elution should be improved for the application of organo lead halide perovskite solar cells.
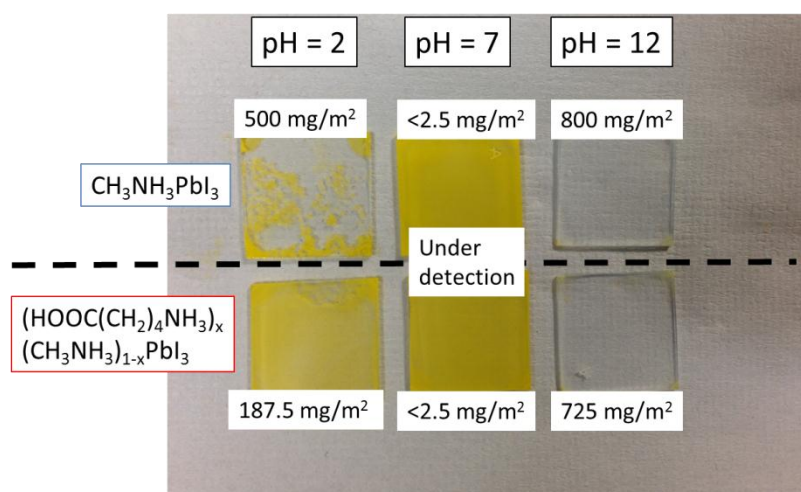

Figure 6. Pictures of the one-step-processed $CH_3NH_3PbI_3$ perovskite layers with/without 5-aminovaleric acid (5AVA) doping, dipped in water, aqueous HCl solution (pH = 2) and aqueous NaOH solution (pH = 12). The numbers inserted in the picture show the amount of the lead dissolved into the water, the aqueous HCl solution (pH = 2) and the aqueous NaOH solution (pH = 12).

Figure 7 shows a summary of the reaction image between the $CH_3NH_3PbI_3$ perovskite crystal for the deposition of solvents (chlorobenzene and propyl sulfide) and HTM (spiro-OMeTAD and CuSCN). Chlorobenzene can extract DMF in the non-dried perovskite layer [14]. Moreover, the chlorobenzene may have a similar effect on the annealed perovskite layer (from Figure 1). In contrast, propyl sulfide did not shift the peak position, but decreased the intensity due to the decomposing of the smaller crystal (from Figure 1). The thiocyanate ion (SCN^-) can be exchanged by the iodide ion (I^-) in PbI_2 [15] and by the chloride (Cl^-) and bromide (Br^-) ions doped in perovskite crystals to be $CH_3NH_3Pb(SCN)_2I$ perovskite [15], resulting in the prevention of the CuSCN crystal on the $CH_3NH_3PbI_3$ perovskite layer (from Figures 2–4). The Cu^+ ion and the SCN^- ion can enhance the crystallinity of $CH_3NH_3PbI_3$ perovskite. However, the chloride ion and the excess amount of I^- (from PbI_2) can suppress the enhancement of the $CH_3NH_3PbI_3$ perovskite crystallinity. For the 2D $(5-AVA)_x(CH_3NH_3)_{1-x}PbI_3$ perovskite crystal, the lithium ion and TBP in spiro-OMeTAD HTM can be inserted between the layered

perovskite crystal (as in Figure 7b, from Figure 5). The deposition of CuSCN HTM can convert the 2D crystal to a 3D one.

In order to discuss the $CH_3NH_3PbI_3$ perovskite crystal transformation, the water content (purity) in the solvents, HTM materials and atmosphere should be explained, because water can decompose the $CH_3NH_3PbI_3$ perovskite crystal into PbI_2 ([16]; as in Figure 6). In this work, the humidity of the laboratory was 60% to 80%. The contents of water in the HTM materials and the solvents were not measured. However, the HTM depositions did not enhance the PbI_2 peak during the experiments, basically (only one exception was the two-step-processed $CH_3NH_3PbI_3$ perovskite with CuSCN HTM in Figure 3). Therefore, it is considered that the effect of water can be negligible. For the further study of the stability of perovskite solar cells, the amount of water in HTM would be very important.
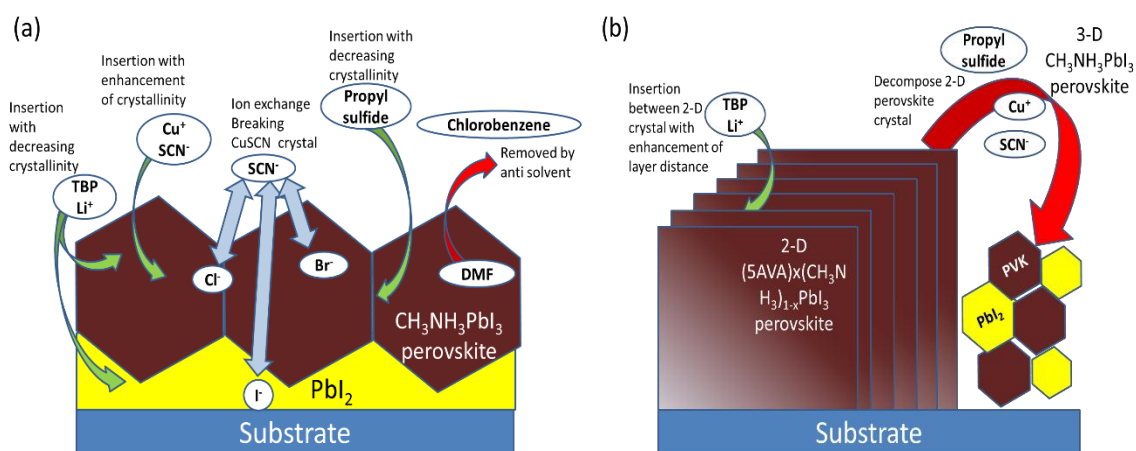

Figure 7. Summary of the reaction scheme of organo lead halide perovskite layers for $CH_3NH_3PbX_3$ (X: I, Cl or Br) (**a**) and for $(HOOC(CH_2)_4NH_3)_x(CH_3NH_3)_{1-x}PbI_3$ (**b**).

Moreover, some molecules (DMF, DMSO, *etc.*) were known to be inserted into the crystal lattice, as studied by Yang *et al.* [5]. In this work, the experiments had been performed in laboratory fume hoods. No glovebox was used for the experiments. Hence, it was considered that the effect of volatile solvent on the perovskite surface from air was eliminated effectively. Of course, there is a chance that the changes by solvent exposure are irreversible or returned (recovered) after annealing of the perovskite layer, as reported by Jeon *et al.* [17], which is generally carried out for the completion of a stand-alone perovskite layer. However, the aim of this paper is to show the instability against HTM deposition, which will not be annealed after the HTM deposition. Moreover, Cu^{2+}, SCN^- and Li^+ are non-volatile ions. Hence, we would like to skip the annealing effect of crystal recovery after HTM deposition for future studies.

The decomposition mechanism of the $CH_3NH_3PbI_3$ perovskite crystal by the lithium ion and TBP was speculated as the exchanging effect with the methyl ammonium ion ($CH_3NH_3^+$). Basically, TBP is a strong base, which can exchange H^+ with water or $CH_3NH_3^+$. In contrast, it can be speculated that the lithium ion and TBP can be inserted into the hydrogen bonding (R-COOH $\cdots$ HOOC-R; the dot line "$\cdots$" represents hydrogen bonding) in the gap between the 5-AVA-ion ($HOOC(CH_2)_4NH_3^+$)-doped 2D perovskite crystals. Further research will be performed to elucidate the exact mechanism.

4. Conclusion

In conclusion, the effect of HTM deposition on the $CH_3NH_3PbI_3$ perovskite crystal was systematically investigated by XRD. It was confirmed that although inorganic HTM can work effectively as organic HTM, CuSCN can react with $CH_3NH_3PbI_3$. Therefore, porous TiO_2 is necessary to block short circuits [9]. In order to achieve concrete results, further experiments should be done, for example TEM, XPS, SEM, Auger spectroscopy, X-ray absorption fine structure (XASF), and so on. However, it is quite important to show the preliminary results and to investigate the inside of the $CH_3NH_3PbI_3$ perovskite crystal. It can be concluded that the $CH_3NH_3PbI_3$ perovskite crystal is too soft and flexible to be stabilized against HTM deposition. In order to enhance the perovskite-crystal crystallinity and stability, the mixed halogen effect and 2D perovskite have been published [10–12]. However, no method for them can enhance the crystal stability. For the further application of $CH_3NH_3PbI_3$ perovskite solar cells, the migration of HTM materials to the perovskite layer should be considered, because such post-deposition of HTM can decompose the soft perovskite crystal. Therefore, the perovskite crystal should be deposited as the last material deposited in the perovskite solar cells. For example, the structure of full-printed solar cells as, <FTO/compact-TiO_2/porous-TiO_2/

porous-ZrO_2/(porous-NiO)/porous-carbon (perovskite was inserted into the porous electrodes)> is quite promising, because the perovskite crystal can be formed at the end of the process [12,18].

Author Contributions

S.I. conceived and designed the experiments, and wrote the paper; S.K. performed the experiments; H.N. contributed the discussions; T.U. and H.I. provided tris(2-(1H-pyrazol-1-yl)-4-*tert*-butylpyridine)cobalt(III) tris(bis(trifluoromethylsulfonyl) imide.

Conflicts of Interest

The authors declare no conflict of interest.

References

1. Kojima, A.; Teshima, K.; Shirai, Y.; Miyasaka, T. Organometal halide perovskites as visible-light sensitizers for photovoltaic cells. *J. Am. Chem. Soc.* **2009**, *131*, 6050–6051.
2. Im, J.-H.; Lee, C.-R.; Lee, J.-W.; Park, S.-W.; Park, N.-G. 6.5% efficient perovskite quantum-dot-sensitized solar cell. *Nanoscale* **2011**, *3*, 4088–4093.
3. Kim, H.-S.; Lee, C.-R.; Im, J.-H.; Lee, K.-B.; Moehl, T.; Marchioro, A.; Moon, S.-J.; Humphry-Baker, R.; Yum, J.-H.; *et al.* Lead iodide perovskite sensitized all-solid-state submicron thin film mesoscopic solar cell with efficiency exceeding 9%. *Sci. Rep.* **2012**, *2*, 591.

4. Lee, M.M.; Teuscher, J.; Miyasaka, T.; Murakami, T.N.; Snaith, H.J. Efficient hybrid solar cells based on meso-superstructured organometal halide perovskites. *Science* **2012**, *338*, 643−647.

5. Yang, W.S.; Noh, J.H.; Jeon, N.J.; Kim, Y.C.; Ryu, S.; Seo, J.; Seok, S.I. High-performance photovoltaic perovskite layers fabricated through intramolecular exchange. *Science* **2015**, *348*, 1234–1237.

6. Eames, C.; Frost, J.M.; Barnes, P.R.F.; O'Regan, B.C.; Walsh, A.; Islam, M.S. Ionic transport in hybrid lead iodide perovskite solar cells. *Nature Commun.* **2015**, *6*, 7497.

7. Yuan, Y.; Chae, J.; Shao, Y.; Wang, Q.; Xiao, Z.; Centrone, A.; Huang, J. Photovoltaic switching mechanism in lateral structure hybrid perovskite solar cells. *Adv. Energy Mater.* **2015**, doi: 10.1002/aenm.201500615.

8. Peng, Q.; Tanaka, S.; Ito, S.; Tetreault, N.; Manabe, K.; Nishino, H.; Nazeeruddin, M.K.; Grätzel, M. Inorganic hole conductor-based lead halide perovskite solar cells with 12.4% conversion efficiency. *Nature Commun.* **2014**, *5*, 3834.

9. Murugadoss, G.; Mizuta, G.; Tanaka, S.; Nishino, H.; Umeyama, T.; Imahori, H.; Ito, S. Double functions of porous TiO_2 electrodes on $CH_3NH_3PbI_3$ perovskite solar cells: Enhancement of perovskite crystal transformation and prohibition of short circuiting. *APL Mater.* **2014**, *2*, 081511. doi: org/10.1063/1.4891597.

10. Zhao, Y.; Zhu, K. CH_3NH_3Cl-Assisted One-Step Solution Growth of $CH_3NH_3PbI_3$: Structure, charge-carrier dynamics, and photovoltaic properties of perovskite solar cells. *J. Phys. Chem. C* **2014**, doi:10.1021/jp502696w.

11. Noh, J.H.; Im, S.H.; Heo, J.H.; Mandal, T.N.; Seok, S.I. Chemical management for colorful, efficient, and stable inorganic-organic hybrid nanostructured solar cells. *Nano Lett.* **2013**, *13*, 1764–1769.

12. Mei, A.; Li, X.; Liu, L.; Ku, Z.; Liu, T.; Rong, Y.; Xu, M.; Hu, M.; Chen, J.; Yang, Y.; *et al.* A hole-conductor–free, fully printable mesoscopic perovskite solar cell with high stability. *Science* **2014**, *345*, 295–298.

13. Burschka, J.; Pellet, N.; Moon, S.-J.; Humphry-Baker, R.; Gao, P.; Nazeeruddin, M.K.; Grätzel, M. Sequential deposition as a route to high-performance perovskite-sensitized solar cells. *Nature* **2013**, *499*, 316−319.

14. Xiao, M.; Huang, F.; Huang, W.; Dkhissi, Y.; Zhu, Y.; Etheridge, J.; Gray-Weale, A.; Bach, U.; Cheng, Y.-B.; Spiccia, L. A fast deposition-crystallization procedure for highly efficient lead iodide perovskite thin-film solar cells. *Angew. Chem. Int. Ed.* **2014**, *53*, 9898–9903.

15. Jiang, Q.; Rebollar, D.; Gong, J.; Piacentino, E.L.; Zheng, C.; Xu, T. Pseudohalide-induced moisture tolerance in perovskite $CH_3NH_3Pb(SCN)_2I$ Thin Films. *Angew. Chem. Int. Ed.* **2015**, doi:10.1002/anie.201503038.

16. Smith, I.C.; Hoke, E.T.; Solis-Ibarra, D.; McGehee, M.D.; Karunadasa, H.I. A layered hybrid perovskite solar-cell absorber with enhanced moisture stability. *Angew. Chem. Int. Ed.* **2014**, *53*, doi:10.1002/anie.201406466.

17. Jeon, N.J.; Noh, J.H.; Kim, Y.C.; Yang, W.S.; Ryu, S.; Seok, S.I. Solvent engineering for high-performance inorganic-organic hybrid perovskite solar cells. *Nat. Mater.* **2014**, *13*, 897–903.

18. Xu, X.; Liu, Z.; Zuo, Z.; Zhang, M.; Zhao, Z.; Shen, Y.; Zhou, H.; Chen, Q.; Yang, Y.; Wang, M. Hole selective NiO contact for efficient perovskite solar cells with carbon electrode. *Nano Lett.* **2015**, *15*, 2402−2408.